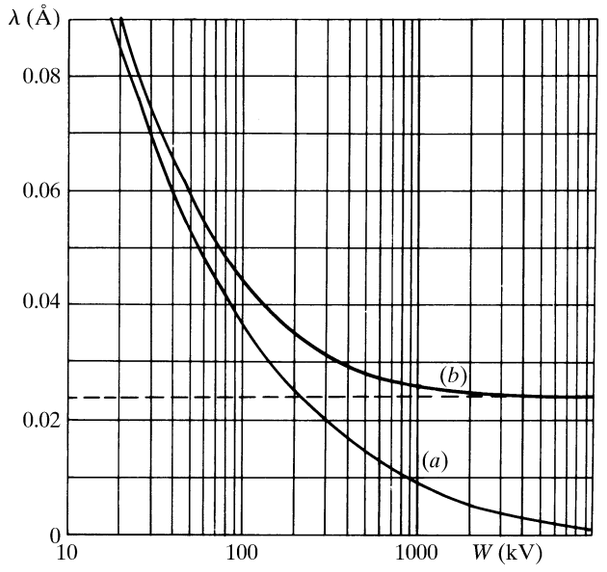

Fig. 2.5.2.1. The variation with accelerating voltage of electrons of (*a*) the wavelength, λ and (*b*) the quantity $\lambda[1 + (h^2/m_0^2c^2\lambda^2)] = \lambda_c/\beta$ which is proportional to the interaction constant σ [equation (2.5.2.14)]. The limit is the Compton wavelength λ_c (after Fujiwara, 1961).

$$\psi(\mathbf{r}) = \exp\{-i\mathbf{k}_0 \cdot \mathbf{r}\} + i\frac{\exp\{-i\mathbf{k} \cdot \mathbf{r}\}}{R\lambda}\sigma f(\mathbf{u}),$$
$$f(\mathbf{u}) = \int \varphi(\mathbf{r}) \exp\{2\pi i\mathbf{u} \cdot \mathbf{r}\}\, \mathrm{d}\mathbf{r}. \qquad (2.5.2.10)$$

For centrosymmetrical atom potential distributions, the $f(\mathbf{u})$ are real, positive and monotonically decreasing with $|\mathbf{u}|$. A measure of the extent of the validity of the first Born approximation is given by the fact that the effect of adding the higher-order terms of the Born series may be represented by replacing $f(\mathbf{u})$ in (2.5.2.10) by the complex quantities $f(\mathbf{u}) = |\mathbf{f}| \exp\{i\eta(\mathbf{u})\}$ and for single heavy atoms the phase factor η may vary from 0.2 for $|\mathbf{u}| = 0$ to 4 or 5 for large $|\mathbf{u}|$, as seen from the tables of *IT* C (2004, Section 4.3.3).

(6) Relativistic effects produce appreciable variations of the parameters used above for the range of electron energies considered. The relativistic values are

$$m = m_0(1 - v^2/c^2)^{-1/2} = m_0(1 - \beta^2)^{-1/2}, \qquad (2.5.2.11)$$
$$\lambda = h[2m_0|e|W(1 + |e|W/2m_0c^2)]^{-1/2} \qquad (2.5.2.12)$$
$$= \lambda_c(1 - \beta^2)^{1/2}/\beta, \qquad (2.5.2.13)$$

where λ_c is the Compton wavelength, $\lambda_c = h/m_0c = 0.0242$ Å, and

$$\sigma = 2\pi me\lambda/h^2 = (2\pi m_0 e/h^2)(\lambda_c/\beta)$$
$$= 2\pi/\{\lambda W[1 + (1 - \beta^2)^{1/2}]\}. \qquad (2.5.2.14)$$

Values for these quantities are listed in *IT* C (2004, Section 4.3.2). The variations of λ and σ with accelerating voltage are illustrated in Fig. 2.5.2.1. For high voltages, σ tends to a constant value, $2\pi m_0 e\lambda_c/h^2 = e/\hbar c$.

2.5.2.3. Recommended sign conventions

There are two alternative sets of signs for the functions describing wave optics. Both sets have been widely used in the literature. There is, however, a requirement for internal consistency within a particular analysis, independently of which set is adopted. Unfortunately, this requirement has not always been met and, in fact, it is only too easy at the outset of an analysis to make errors in this way. This problem might have come into prominence somewhat earlier were it not for the fact that, for centrosymmetric crystals (or indeed for centrosymmetric projections in the case of planar diffraction), only the signs used in the transmission and propagation functions can affect the results. It is not until the origin is set away from a centre of symmetry that there is a need to be consistent in every sign used.

Signs for electron diffraction have been chosen from two points of view: (1) defining as positive the sign of the exponent in the structure-factor expression and (2) defining the forward propagating free-space wavefunction with a positive exponent.

The second of these alternatives is the one which has been adopted in most solid-state and quantum-mechanical texts.

The first, or *standard crystallographic* convention, is the one which could most easily be adopted by crystallographers accustomed to retaining a positive exponent in the structure-factor equation. This also represents a consistent *International Tables* usage. It is, however, realized that both conventions will continue to be used in crystallographic computations, and that there are by now a large number of operational programs in use.

It is therefore recommended (*a*) that a particular sign usage be indicated as either *standard crystallographic* or *alternative crystallographic* to accord with Table 2.5.2.1, whenever there is a need for this to be explicit in publication, and (*b*) that either one or other of these systems be adhered to throughout an analysis in a self-consistent way, even in those cases where, as indicated above, some of the signs appear to have no effect on one particular conclusion.

2.5.2.4. Scattering of electrons by crystals; approximations

The forward-scattering approximation to the many-beam dynamical diffraction theory outlined in Chapter 5.2 provides the basis for the calculation of diffraction intensities and electron-microscope image contrast for thin crystals. [See Cowley (1995), Chapter 5.2 and *IT* C (2004) Sections 4.3.6 and 4.3.8.] On the other hand, there are various approximations which provide relatively simple analytical expressions, are useful for the determination of diffraction geometry, and allow estimates to be made of the relative intensities in diffraction patterns and electron micrographs in favourable cases.

(*a*) *The kinematical approximation*, derived in Section 2.5.2.2 from the first Born approximation, is analagous to the corresponding approximation of X-ray diffraction. It assumes that the scattering amplitudes are directly proportional to the three-dimensional Fourier transform of the potential distribution, $\varphi(\mathbf{r})$.

$$V(\mathbf{u}) = \int \varphi(\mathbf{r}) \exp\{2\pi i\mathbf{u} \cdot \mathbf{r}\}\, \mathrm{d}\mathbf{r}, \qquad (2.5.2.15)$$

so that the potential distribution $\varphi(\mathbf{r})$ takes the place of the charge-density distribution, $\rho(\mathbf{r})$, relevant for X-ray scattering.

The validity of the kinematical approximation as a basis for structure analysis is severely limited. For light-atom materials, such as organic compounds, it has been shown by Jap & Glaeser (1980) that the thickness for which the approximation gives reasonable accuracy for zone-axis patterns from single crystals is of the order of 100 Å for 100 keV electrons and increases, approximately as σ^{-1}, for higher energies. The thickness limits quoted for polycrystalline samples, having crystallite dimensions smaller than the sample thickness, are usually greater (Vainshtein, 1956). For heavy-atom materials the approximation is more limited since it may fail significantly for single heavy atoms.

(*b*) *The phase-object approximation* (POA), or high-voltage limit, is derived from the general many-beam dynamical

Table 2.5.2.1. *Standard crystallographic and alternative crystallographic sign conventions for electron diffraction*

	Standard	Alternative
Free-space wave	$\exp[-i(\mathbf{k}\cdot\mathbf{r}-\omega t)]$	$\exp[+i(\mathbf{k}\cdot\mathbf{r}-\omega t)]$
Fourier transforming from real space to reciprocal space	$\int \psi(\mathbf{r})\exp[+2\pi i(\mathbf{u}\cdot\mathbf{r})]\,\mathrm{d}\mathbf{r}$	$\int \psi(\mathbf{r})\exp[-2\pi i(\mathbf{u}\cdot\mathbf{r})]\,\mathrm{d}\mathbf{r}$
Fourier transforming from reciprocal space to real space	$\psi(\mathbf{r}) = \int \Psi(\mathbf{u})\exp[-2\pi i(\mathbf{u}\cdot\mathbf{r})]\,\mathrm{d}\mathbf{u}$	$\int \Psi(\mathbf{u})\exp[+2\pi i(\mathbf{u}\cdot\mathbf{r})]\,\mathrm{d}\mathbf{u}$
Structure factors	$V(\mathbf{h}) = (1/\Omega)\sum_j f_j(\mathbf{h})\exp(+2\pi i\mathbf{h}\cdot\mathbf{r}_j)$	$(1/\Omega)\sum_j f_j(\mathbf{h})\exp(-2\pi i\mathbf{h}\cdot\mathbf{r}_j)$
Transmission function (real space)	$\exp[-i\sigma\varphi(x,y)\Delta z]$	$\exp[+i\sigma\varphi(x,y)\Delta z]$
Phenomenological absorption	$\sigma\varphi(\mathbf{r}) - i\mu(\mathbf{r})$	$\sigma\varphi(\mathbf{r}) + i\mu(\mathbf{r})$
Propagation function $P(h)$ (reciprocal space) within the crystal	$\exp(-2\pi i\zeta_{\mathbf{h}}\Delta z)$	$\exp(+2\pi i\zeta_{\mathbf{h}}\Delta z)$
Iteration (reciprocal space)	$\Psi_{n+1}(\mathbf{h}) = [\Psi_n(\mathbf{h})\cdot P(\mathbf{h})] * Q(\mathbf{h})$	
Unitarity test (for no absorption)	$T(\mathbf{h}) = Q(\mathbf{h}) * Q^*(-\mathbf{h}) = \delta(\mathbf{h})$	
Propagation to the image plane-wave aberration function, where $\chi(U) = \pi\lambda\Delta f U^2 + \frac{1}{2}\pi C_s\lambda^3 U^4$, $U^2 = u^2 + v^2$ and Δf is positive for overfocus	$\exp[i\chi(U)]$	$\exp[-i\chi(U)]$

σ = electron interaction constant $= 2\pi me\lambda/h^2$; m = (relativistic) electron mass; λ = electron wavelength; e = (magnitude of) electron charge; h = Planck's constant; $k = 2\pi/\lambda$; Ω = volume of the unit cell; $\mathbf{u}$ = continuous reciprocal-space vector, components u, v; $\mathbf{h}$ = discrete reciprocal-space coordinate; $\varphi(x, y)$ = crystal potential averaged along beam direction (positive); Δz = slice thickness; $\mu(\mathbf{r})$ = absorption potential [positive; typically $\leq 0.1\sigma\varphi(\mathbf{r})$]; Δf = defocus (defined as negative for underfocus); C_s = spherical aberration coefficient; $\zeta_{\mathbf{h}}$ = excitation error relative to the incident-beam direction and defined as negative when the point h lies outside the Ewald sphere; $f_j(\mathbf{h})$ = atomic scattering factor for electrons, f_e, related to the atomic scattering factor for X-rays, f_X, by the Mott formula $f_e = (e/\pi U^2)(Z - f_X)$. $Q(\mathbf{h})$ = Fourier transform of periodic slice transmission function.

diffraction expression, equation (5.2.13.1), Chapter 5.2, by assuming the Ewald sphere curvature to approach zero. Then the scattering by a thin sample can be expressed by multiplying the incoming wave amplitude by the transmission function

$$q(xy) = \exp\{-i\sigma\varphi(xy)\}, \tag{2.5.2.16}$$

where $\varphi(xy) = \int \varphi(\mathbf{r})\,\mathrm{d}z$ is the projection of the potential distribution of the sample in the z direction, the direction of the incident beam. The diffraction-pattern amplitudes are then given by two-dimensional Fourier transform of (2.5.2.16).

This approximation is of particular value in relation to the electron microscopy of thin crystals. The thickness for its validity for 100 keV electrons is within the range 10 to 50 Å, depending on the accuracy and spatial resolution involved, and increases with accelerating voltage approximately as $\lambda^{-1/2}$. In computational work, it provides the starting point for the multislice method of dynamical diffraction calculations (*IT* C, 2004, Section 4.3.6.1).

(*c*) *The two-beam approximation* for dynamical diffraction of electrons assumes that only two beams, the incident beam and one diffracted beam (or two Bloch waves, each with two component amplitudes), exist in the crystal. This approximation has been adapted, notably by Hirsch *et al.* (1965), for use in the electron microscopy of inorganic materials.

It forms a convenient basis for the study of defects in crystals having small unit cells (metals, semiconductors *etc.*) and provides good preliminary estimates for the determination of crystal thicknesses and structure amplitudes for orientations well removed from principal axes, and for electron energies up to 200–500 keV, but it has decreasing validity, even for favourable cases, for higher energies. It has been used in the past as an 'extinction correction' for powder-pattern intensities (Vainshtein, 1956).

(*d*) *The Bethe second approximation*, proposed by Bethe (1928) as a means for correcting the two-beam approximation for the effects of weakly excited beams, replaces the Fourier coefficients of potential by the 'Bethe potentials'

$$U_{\mathbf{h}} = V_{\mathbf{h}} - 2k_0\sigma\sum_{\mathbf{g}}\frac{V_{\mathbf{g}}\cdot V_{\mathbf{h}-\mathbf{g}}}{\kappa^2 - k_{\mathbf{g}}^2}. \tag{2.5.2.17}$$

Use of these potentials has been shown to account well for the deviations of powder-pattern intensities from the predictions of two-beam theory (Horstmann & Meyer, 1965) and to predict accurately the extinctions of Kikuchi lines at particular accelerating voltages due to relativistic effects (Watanabe *et al.*, 1968), but they give incorrect results for the small-thickness limit.

2.5.2.5. Kinematical diffraction formulae

(1) *Comparison with X-ray diffraction.* The relations of real-space and reciprocal-space functions are analogous to those for X-ray diffraction [see equations (2.5.2.2), (2.5.2.10) and (2.5.2.15)]. For diffraction by crystals

$$\varphi(\mathbf{r}) = \sum_{\mathbf{h}} V_{\mathbf{h}}\exp\{-2\pi i\mathbf{h}\cdot\mathbf{r}\},$$

$$V_{\mathbf{h}} = \int \varphi(\mathbf{r})\exp\{2\varphi i\mathbf{h}\cdot\mathbf{r}\}\,\mathrm{d}\mathbf{r} \tag{2.5.2.18}$$

$$= \frac{1}{\Omega}\sum_i f_i(\mathbf{h})\exp\{2\pi i\mathbf{h}\cdot\mathbf{r}_i\}, \tag{2.5.2.19}$$

where the integral of (2.5.2.18) and the summation of (2.5.2.19) are taken over one unit cell of volume (see Dawson *et al.*, 1974).

Important differences from the X-ray case arise because

(*a*) the wavelength is relatively small so that the Ewald-sphere curvature is small in the reciprocal-space region of appreciable scattering amplitude;

(*b*) the dimensions of the single-crystal regions giving appreciable scattering amplitudes are small so that the 'shape transform' regions of scattering power around the reciprocal-lattice points are relatively large;

(*c*) the spread of wavelengths is small (10^{-5} or less, with no white-radiation background) and the degree of collimation is better (10^{-4} to 10^{-6}) than for conventional X-ray sources.

As a consequence of these factors, single-crystal diffraction patterns may show many simultaneous reflections, representing almost-planar sections of reciprocal space, and may show fine structure or intensity variations reflecting the crystal dimensions and shape.

(2) Kinematical diffraction-pattern intensities are calculated in a manner analogous to that for X-rays except that

(*a*) no polarization factor is included because of the small-angle scattering conditions;

(*b*) integration over regions of scattering power around reciprocal-lattice points cannot be assumed unless appropriate experimental conditions are ensured.

For a thin, flat, lamellar crystal of thickness H, the observed intensity is